Soil Dynamics and Earthquake Engineering 33 (2012) 38–53

Contents lists available at SciVerse ScienceDirect

Soil Dynamics and Earthquake Engineering

journal homepage: www.elsevier.com/locate/soildyn

Dynamic properties of dry sand/rubber (SRM) and gravel/rubber (GRM) mixtures in a wide range of shearing strain amplitudes

Kostas Senetakis [a,*,1], Anastasios Anastasiadis [b], Kyriazis Pitilakis [b]

[a] Department of Civil and Architectural Engineering, City University of Hong Kong, Hong Kong
[b] Department of Civil Engineering, Aristotle University of Thessaloniki, Greece

ARTICLE INFO

Article history:
Received 31 May 2011
Received in revised form
5 October 2011
Accepted 7 October 2011
Available online 28 October 2011

Keywords:
Recycled geomaterials
Geosynthetics
Sand/rubber mixtures
Gravel/rubber mixtures
Shear modulus
Damping ratio
Strain-dependent dynamic properties
Resonant column test

ABSTRACT

Recycled tire rubber in mixtures with granular soils has been found recently applications in many civil engineering projects. The paper presents a synthesis of the dynamic strain-dependent properties of the commonly used soil/rubber mixtures, which are necessary in any seismic design. We focus herein on high-amplitude resonant column tests on granular soil/rubber mixtures with varying percentage of rubber. The most important characteristics of the dynamic properties of the mixtures like the confining pressure, the content of rubber, the grain-size characteristics of the physical portion of the mixtures as well as the relative size of soil versus rubber solids, are thoroughly discussed. We propose generic normalized shear modulus and damping ratio versus shearing strain amplitude curves for dry mixtures of sand/rubber (SRM) and gravel/rubber (GRM) appropriate for the engineering practice. Finally, we summarize analytical expressions for small-strain shear modulus and damping ratio for SRM and GRM proposed in previous studies.

1. Introduction

The pressing environmental need of recycling waste automobile tires led the civil engineering research community on contriving ways to re-use these materials in an innovative manner. The last two decades in many geotechnical projects all over the world, recycled rubber poor or mixed with granular soils as well as tire balls, have been utilized as lightweight construction, fill, drainage or thermal-isolation material [1–7]. Recycled tires in granulated or shredded form exhibit frictional behavior, low unit weight of solids, low bulk density, high hydraulic conductibility and high elastic deformability [6,8–11]. Mixtures of soils with relatively low to medium rubber content ($\leq 35\%$ per weight or $\leq 55\%$ per volume) exhibit a reduction of void ratio with increasing the inclusion of rubber, that is a more dense fabric of the soil/rubber solid matrix, high shear strength and low to medium compressibility [11–21].

Furthermore, due to the interesting dynamic response of granulated rubber or tire shreds, that is high linearity in the region of medium to high strains and high damping, mixtures of sand/rubber (SRM) and gravel/rubber (GRM) comprise potential attenuation vibration materials for the mitigation of earthquake-induced loads on infrastructures. Recent results stemming from shaking table and cyclic triaxial tests [22–25] as well as from numerical studies [26–31] have shown promising results on the use of recycled rubber pure or in mixtures with granular soils, as isolation backfill material on retaining walls, underground layer for the mitigation of liquefaction phenomena, or even isolation system for buildings.

According to the available data and concerning small to relatively medium rubber contents, SRM and GRM exhibit strain-dependent behavior under cyclic-dynamic loads [29,32–36] and thus, the dynamic response of a structure strongly depends on the dynamic properties (i.e. G_O and G/G_O–log γ–DT curves) of the SRM/GRM material used as construction, backfill or foundation material. Consequently, the knowledge of the dynamic, strain-dependent properties of the SRM/GRM is compulsory for the safe seismic design of a structure.

In this paper, we synthesize past [29,33–35] and recently acquired [36] high-amplitude resonant column test results, in order (a) to study the most important parameters affecting the dynamic behavior of sand/rubber (SRM) and gravel/rubber (GRM) mixtures, (b) to develop generic G/G_O–log γ–DT curves for SRM and GRM filling in that way the literature gap concerning the strain-dependent dynamic properties of the aforementioned complex materials.

All experiments in this paper were performed in the Laboratory of Soil Mechanics, Foundations and Geotechnical Earthquake

* Corresponding author.
E-mail addresses: ksenetak@civil.auth.gr (K. Senetakis), anas@civil.auth.gr (A. Anastasiadis), kpitilak@civil.auth.gr (K. Pitilakis).
[1] Formerly at Aristotle University of Thessaloniki, Greece.

0267-7261/$ - see front matter © 2011 Elsevier Ltd. All rights reserved.
doi:10.1016/j.soildyn.2011.10.003

Engineering of Aristotle University in Thessaloniki, Greece. We focus herein on dry mixtures of high relative density specimens of approximately 71.1 mm diameter and 142.2 mm height and small to relatively medium rubber contents ranging from 0% to 35% by mixture weight. The effect of specimens geometry, conditions of saturation and creep phenomena on the dynamic behavior of SRM have been recently discussed by Anastasiadis et al. [37] and Senetakis et al. [34] in which analytical relationships for the estimation of shear modulus and damping ratio of dry and saturated mixtures were also presented. The parent granular materials in these works were composed of uniform, fine to medium grained sands. In the present paper these past experimental works have been completed for coarse sand/rubber and gravel/rubber mixtures including the effect of the coefficient of uniformity of the physical portion of the mixtures as well as the effect of the relative size of soil particles versus rubber solids, and the analytical expressions for the estimation of shear modulus and damping ratio as a function of shearing strain amplitude proposed by Senetakis et al. [34] are generalized for a wider range of coarse sands and gravelly soil mixed with granulated rubber materials of variable mean grain size. In addition, we summarize herein the analytical expressions for the estimation of small-strain shear modulus and damping ratio of SRM and GRM proposed by Anastasiadis et al. [38] and Senetakis [36].

2. Materials tested, sample preparation and testing program

2.1. 'Parent' materials

Tables 1 and 2 summarize the 'parent' materials used as physical and synthetic-rubber part of the mixtures tested. Three of the physical materials were constructed using a fluvial sand of sub-rounded to rounded particles, namely C2D03, C3D06 and C2D1. Four of the physical materials were constructed using a quarry sandy gravel of sub-angular to angular particles, namely C2D3, C6D3, C13D3 and C1D8. According to ASTM specification [39] the 'parent' granular materials are classified as SP, SP-SW and GP, exhibiting a mean grain size of solids (D_{50}) in a range of 0.30–8.0 mm and a coefficient of uniformity (C_u) in a range of 1.0–13, approximately.

In addition, four uniform rubber materials were used as synthetic part of the mixtures, namely R03, R06, R2 and R3. According to ASTM specification [40] these materials are classified as granulated or particulate rubber, exhibiting a mean grain size (D_{50}) in a range of 0.30–3.0 mm and a coefficient of uniformity (C_u) in a range of 2.0–3.0, approximately.

Figs. 1 and 2 depict the grain size distribution curves of the 'parent' materials used. The specific gravity (G_s) of soil and rubber solids in materials C2D03, C3D06, C2D3, R06 and R3 was determined following the ASTM specification [41]; soil particles exhibit a value $G_s=2.67$ g/cm^3, whereas rubber solids exhibit a value $G_s=1.10$ g/cm^3.

2.2. Experimental equipment, preparation of specimens

The cyclic tests were performed in a fixed-free longitudinal-torsional resonant column (RC) device [42]. In this apparatus, specimens of 35.7 or 71.1 mm diameter and a height twice the diameter may be tested. The bottom-passive end of the specimens is rigidly fixed on a base pedestal of mass and inertia significantly greater in comparison to the corresponding mass and inertia of the specimens tested, whereas the sinusoidal excitation is applied at the top-active end using two magnets embodied at the excitation mechanism and four coils that surround the magnets

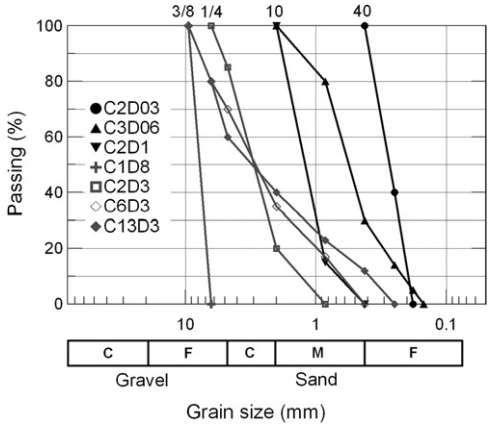

Fig. 1. Grain-size distribution curves of 'parent' sandy and gravelly soils.

Table 2
'Parent' rubber materials used as synthetic part of the mixtures ($G_s=1.10$ g/cm^3).

No.	Code name of material	Classification[a]	D_{max} (mm)	D_{50} (mm)	C_u[b]	C_c[c]
1	R03	Granulated rubber	0.85–2.00	0.34	1.95	0.87
2	R06	Granulated rubber	2.00–4.75	0.40	2.65	0.85
3	R2	Granulated rubber	2.00–4.75	1.50	1.81	0.96
4	R3	Granulated rubber	4.75–6.35	2.80	2.29	1.18

[a] [40].
[b] $C_u=D_{60}/D_{10}$.
[c] $C_c=D_{30}^2/(D_{60}\times D_{10})$.

Table 1
'Parent' sandy and gravelly soils used as physical part of the mixtures ($G_s=2.67$ g/cm^3).

No.	Code name of material	Initial soil	Classification[a]	Gravel content (%)	D_{max} (mm)	D_{50}(mm)	C_u[b]	C_c[c]
1	C2D03	Fluvial sand[d]	SP	0	0.25–0.43	0.27	1.58	0.93
2	C3D06	Fluvial sand	SP	0	0.85–2.00	0.56	2.76	1.23
3	C2D1	Fluvial sand	SP	0	0.85–2.00	1.33	2.13	1.01
4	C2D3	Quarry sandy gravel[e]	SP	15	4.75–6.35	3.00	2.45	1.10
5	C1D8	Quarry sandy gravel	GP	100	6.35–9.53	7.80	1.22	0.94
6	C6D3	Quarry sandy gravel	SP-SW	30	6.35–9.53	2.90	5.95	1.19
7	C13D3	Quarry sandy gravel	SP-SW	40	6.35–9.53	3.00	12.50	0.94

[a] [39].
[b] $C_u=D_{60}/D_{10}$.
[c] $C_c=D_{30}^2/(D_{60}\times D_{10})$.
[d] Sub-rounded to rounded particles.
[e] Sub-angular to angular particles.

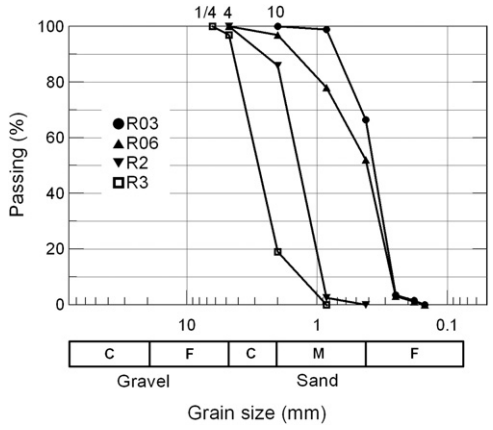

Fig. 2. Grain-size distribution curves of 'parent' granulated rubber materials.

and the top end of the specimen. The resonance of the system is achieved by controlling the excitation frequency until the velocity at the active end is 180° out of phase with the applied force. The torsional resonant column tests and the analysis of the results were performed according to ASTM specification [43].

At a first step, soil and rubber parts were dry mixed in selected percentages of rubber ranging from 0% (clean soils) to 35% by mixture weight, in order to prepare uniform mixtures of specific rubber content. At a second step, 71.1×142.2 mm specimens were constructed in dry conditions into the RC device using a metal mold. In order to construct specimens of high relative density, all specimens were prepared in fourteen layers of equal dry mass, and each layer was compacted in many tips using a small-diameter metal rod. All specimens of clean soils and soil/rubber mixtures were constructed at about the same compaction energy.

Special issues and further details regarding the experimental equipment, the preparation of the mixtures and the construction of the specimens followed herein have been presented in [35–38].

It is also noticed at this point that we limited this study on mixtures with maximum rubber content equal to 35% by weight (which corresponds to about 55–60% rubber content by mixture volume) because it has been reported in the literature that for rubber content above 60% by weight, the mixtures exhibit in general rubber-like behavior; this is mainly due to the predominant development of rubber-to-rubber interfaces and thus the overall static and dynamic response of the mixtures with rubber content above 60% by mixture volume is mainly controlled by the rubber part [20]. In these cases, the mixtures exhibit high compressibility, low shear strength [11,18,20,36] and in general special recommendations (on the design and construction stage) should be followed [40] when clean rubber or mixtures with rubber-like behavior are applied in geo-structures.

2.3. Testing program

Fourty-one dry specimens of seven clean soils (0% rubber content) and thirty-four SRM and GRM (rubber content in a range of 5–35% by mixture weight) were tested using the seven granular soils and the four rubber materials presented in Tables 1 and 2. Low and high amplitude torsional resonant column (RC) tests were performed in a range of shearing strain amplitudes (γ) from about 2×10^{-4}% to 3×10^{-1}% and mean confining pressures (σ'_m) from 25 to 400 kPa. At each confining pressure specimens were allowed to equilibrate about 60–80 min before the performance of low and high amplitude RC tests. This time period was sufficient in most specimens for small-strain resonant frequency ($f_{n,LA}$) to stabilize. After the completion of high-amplitude measurements at a specific σ'_m, specimens were allowed about 30–40 min to equilibrate before the application of the following confining pressure level. This time period was also sufficient in most specimens to recover at least 95% of their small-strain shear modulus.

Table 3
High-amplitude torsional RC testing program.

No.	Mixture group	$D_{50,s}/D_{50,r}$[a]	Rubber content by mixture weight (%)					
			0	5	10	15	25	35
1	C2D03-R3[b]	1:10	●	●	●	●	●	●
2	C2D03-R03	1:1		●		●	●	
3	C3D06-R3	1:5	●	●	●	●	●	●
4	C2D1-R3	1:2	●			●	●	●
5	C2D3-R3	1:1	●	●	●	●	●	●
6	C2D3-R06	5:1		●		●	●	
7	C1D8-R2	5:1	●	●		●	●	
8	C6D3-R3	1:1	●	●		●		●
9	C13D3-R3	1:1	●	●		●	●	●

[a] Ratio of mean grain size of soil versus rubber solids.
[b] 'Parent' soil: C2D03, 'Parent' rubber: R3.

In Table 3, the fourty-one specimens are categorized in nine mixture groups according to the 'parent' soil and the rubber material used in each mixture. For example, mixture group C2D03-R3 is composed of the fine-grained sand C2D03 (see Table 1) and the coarse rubber R3 (see Table 2), while the tested specimens of this mixture group comprise contents of rubber equal to 0%, 5%, 10%, 15%, 25% and 35% by mixture weight. In addition, Table 3 depicts the ratio of mean grain size of soil solids versus rubber solids, $D_{50,s}/D_{50,r}$. Mixtures tested herein exhibit a ratio $D_{50,s}/D_{50,r}$ in a range of 1:10 to 5:1.

The range of mean confining pressure (σ'_m), the initial values of dry unit weight (γ_d) and the bounds of shearing strain amplitude (γ_{LA}) where G_O and DT_O of all specimens are defined are given in Table 4 (G_O and DT_O correspond to the small-strain shear modulus and small-strain damping ratio, respectively).

3. Results and discussion

3.1. Synopsis of the small-strain shear modulus and damping ratio

The effect of rubber content on the small-strain dynamic response of SRM and GRM has been extensively discussed by Anastasiadis et al. [38] and more recently by Senetakis [36]. We summarize herein the analytical equations for the small-strain shear modulus ($G_{O,mix}$) and damping ratio ($DT_{O,mix}$) for SRM and GRM derived from the experimental results.

The small-strain shear modulus ($G_{O,mix}$) is given analytically from Eq. (1) as a function of mean confining pressure (σ'_m) and the corresponding small-strain shear modulus of the mixture at $\sigma'_m = 100$ kPa, $G_{O,mix,100}$. $G_{O,mix,100}$ is given analytically from Eq. (2) as a function of the corresponding small-strain shear modulus of the intact soil having 0% rubber at $\sigma'_m = 100$ kPa, $G_{O,soil,100}$, the ratio $D_{50,s}/D_{50,r}$, where $D_{50,s}$ and $D_{50,r}$ is the mean grain size of soil solids and rubber solids, respectively, and the equivalent void ratio of the mixture at $\sigma'_m = 100$ kPa, $e_{eq,mix,100}$. The constants of Eqs. (1) and (2) (A_G, n_G, A_1, A_2, n_1, n_2) are given in Table 5 separately for mixtures composed of uniform to poor graded soil ($C_{u,s} < 5$) and mixtures composed of well-graded soil ($C_{u,s} > 5$), where $C_{u,s}$ is the coefficient of uniformity of the physical portion of the mixture. In Eqs. (1) and (2), $G_{O,mix}$, $G_{O,mix,100}$ and $G_{O,soil,100}$ are given in MPa, and σ'_m is given in kPa

$$G_{O,mix} = G_{O,mix,100} \times A_G \times (\sigma'_m)^{n_G} \quad (1)$$

Table 4
High-amplitude torsional RC testing program: code names and data of dry 71.1 × 142.2 mm specimens.

No.	Specimen code	Rubber content[a] (%)	γ_d[b] (kN/m^3)	σ_m'[c] (kPa)	γ_{LA}[d] (%)	Ref. code[e]
1	C2D03[f]	0	15.8	50, 100, 200	4.8×10^{-4}–5.2×10^{-4}	[34,35,38,44]
2	C2D03-R3-95/5[g]	5	15.4	50, 100, 200, 400	4.3×10^{-4}–6.7×10^{-4}	[34,35,38]
3	C2D03-R3-90/10	10	14.8	50, 100, 200	8.1×10^{-4}–9.2×10^{-4}	[34,35,38]
4	C2D03-R3-85/15	15	14.2	50, 100, 200, 400	6.9×10^{-4}–8.1×10^{-4}	[34,35,38]
5	C2D03-R3-75/25	25	13.4	50, 100, 200	1.5×10^{-3}–1.6×10^{-3}	[34,35,38]
6	C2D03-R3-65/35	35	12.4	25, 50, 100	1.8×10^{-3}–2.2×10^{-3}	[34,35,38]
7	C2D03-R03-95/5	5	14.6	50, 100, 200	5.4×10^{-4}–6.7×10^{-4}	–
8	C2D03-R03-85/15	15	13.1	50, 100	7.9×10^{-4}–2.1×10^{-3}	–
9	C2D03-R03-75/25	25	11.3	25, 50, 100	2.4×10^{-3}–3.4×10^{-3}	–
10	C3D06[f]	0	16.5	25, 50, 100, 200	4.8×10^{-4}–7.0×10^{-4}	[29,34,44]
11	C3D06-R3-95/5	5	16.4	50, 100, 200	6.2×10^{-4}–7.1×10^{-4}	[29,34]
12	C3D06-R3-90/10	10	15.3	50, 100, 200, 400	1.8×10^{-4}–5.0×10^{-4}	[34]
13	C3D06-R3-85/15	15	14.9	50, 100, 200, 400	3.2×10^{-4}–4.3×10^{-4}	[29,33,34]
14	C3D06-R3-75/25	25	13.9	50, 100, 200, 400	6.9×10^{-4}–9.1×10^{-4}	[34]
15	C3D06-R3-65/35	35	12.6	50, 100, 200	1.1×10^{-3}–1.3×10^{-3}	[33,34]
16	C2D1[f]	0	16.8	50, 100, 200	4.2×10^{-4}–5.6×10^{-4}	[44]
17	C2D1-R3-85/15	15	14.3	50, 100, 200	6.1×10^{-4}–7.8×10^{-4}	–
18	C2D1-R3-75/25	25	13.0	50, 100, 200	2.3×10^{-3}–2.5×10^{-3}	–
19	C2D1-R3-65/35	35	12.4	50, 100, 200, 400	5.2×10^{-3}–5.5×10^{-3}	–
20	C2D3[f]	0	16.3	50, 100	4.0×10^{-4}–4.1×10^{-4}	[44]
21	C2D3-R3-95/5	5	15.4	100, 200	4.0×10^{-4}–4.2×10^{-4}	–
22	C2D3-R3-90/10	10	14.5	50, 100, 200, 400	6.0×10^{-4}–6.8×10^{-4}	–
23	C2D3-R3-85/15	15	13.7	50, 100, 200	5.2×10^{-4}–8.6×10^{-4}	–
24	C2D3-R3-75/25	25	12.6	50, 100, 200, 400	1.4×10^{-3}–1.8×10^{-3}	–
25	C2D3-R3-65/35	35	12.1	50, 100, 200	2.5×10^{-3}–2.7×10^{-3}	–
26	C2D3-R06-95/5	5	16.4	50, 100, 200	1.9×10^{-4}–2.5×10^{-4}	–
27	C2D3-R06-85/15	15	15.4	50, 100	4.8×10^{-4}–4.8×10^{-4}	–
28	C2D3-R06-75/25	25	14.2	50, 100	1.0×10^{-3}–1.4×10^{-3}	–
29	C1D8[f]	0	15.4	25, 50, 100, 200	3.5×10^{-4}–7.2×10^{-4}	[35,44]
30	C1D8-R2-95/5	5	15.6	25, 50, 100, 200	7.4×10^{-4}–9.3×10^{-4}	[35]
31	C1D8-R2-85/15	15	14.9	25, 50, 100	6.2×10^{-4}–7.3×10^{-4}	[35]
32	C1D8-R2-75/25	25	13.8	50, 100, 200	1.5×10^{-3}–1.6×10^{-3}	[35]
33	C6D3[f]	0	17.7	50, 100, 200	2.8×10^{-4}–3.5×10^{-4}	[35]
34	C6D3-R3-95/5	5	16.6	50, 100, 200	2.5×10^{-4}–2.8×10^{-4}	–
35	C6D3-R3-85/15	15	14.3	100, 200, 400	4.4×10^{-4}–4.6×10^{-4}	–
36	C6D3-R3-65/35	35	12.0	100, 200	1.4×10^{-3}–1.5×10^{-3}	–
37	C13D3[f]	0	18.1	50, 100, 200	1.4×10^{-4}–4.4×10^{-4}	[35,44]
38	C13D3-R3-95/5	5	16.9	50, 100, 200	4.4×10^{-4}–5.3×10^{-4}	[35]
39	C13D3-R3-85/15	15	15.3	50, 100, 200	1.1×10^{-3}–1.2×10^{-3}	[35]
40	C13D3-R3-75/25	25	13.7	50, 100	8.5×10^{-4}–2.0×10^{-3}	[35]
41	C13D3-R3-65/35	35	12.7	50, 100	3.8×10^{-3}–4.0×10^{-3}	[35]

[a] By mixture weight.
[b] Initial dry unit weight at $\sigma'_m=25$ kPa.
[c] Mean confining pressure where high-amplitude tests were performed.
[d] Shearing strain amplitude where G_O and DT_O are defined in this study.
[e] Relative papers where representative results or analytical relationships have been presented.
[f] Specimens of clean soils.
[g] Mixture composed of the sand C2D03 and the rubber R3 with 5% rubber content.

Table 5
Parameters for the estimation of the small-strain shear modulus of the SRM and GRM.

No.	Mixture group	A_G	n_G	A_1	A_2	n_1	n_2
1	$C_{u,s}<5$	0.079	0.55	0.3919	2.1365	−0.1602	0.2220
2	$C_{u,s}>5$	0.041	0.69	0.3292	1.7306	−0.1602	0.2220

Note: $C_{u,s}$ is the coefficient of uniformity of the physical part of the mixtures.

Table 6
Parameters for the estimation of the small-strain damping ratio of the SRM and GRM.

No.	Mixture group	A_D	n_D
1	$C_{u,s}<5$	1.750	−0.12
2	$C_{u,s}>5$	2.749	−0.21

$$G_{O,mix,100}=A_1\times G_{O,soil,100}\times\left(\frac{D_{50,s}}{D_{50,r}}\right)^{n_1}\times\frac{1}{e_{eq,mix,100}^{A_2\times(D_{50,s}/D_{50,r})^{n_2}}} \quad (2)$$

The equivalent void ratio, $e_{eq,mix,100}$, is given from Eq. (3) as a function of the void ratio of the intact soil having 0% rubber at the same confining pressure ($\sigma'_m=100$ kPa), $e_{soil,100}$, and the content of rubber (pr) in percentile scale (%). The constants of Eq. (3) are equal to $A_3=0.0008$, $A_4=0.0454$ and $A_5=1$. In equivalent void ratio we treat the volume of rubber solids as part of the total volume of voids, whereas the solids that contribute to the stiffness of the soil/rubber solid matrix are assumed to be the soil particles [32]

$$e_{eq,mix,100}=e_{soil,100}\times(A_3\times pr^2+A_4\times pr+A_5) \quad (3)$$

The small-strain damping ratio ($DT_{O,mix}$) of SRM and GRM is given analytically from Eq. (4) as a function of confining pressure (σ'_m) and the corresponding initial damping ratio of the mixture at $\sigma'_m=100$ kPa, $DT_{O,mix,100}$. $DT_{O,mix,100}$ is correlated with the corresponding small-strain damping ratio of the intact soil having 0% rubber at $\sigma'_m=100$ kPa, $DT_{O,soil,100}$, and a linear function of the content of rubber, $F(pr_d)$, through Eq. (5). The function $F(pr_d)$ is given in Eq. (6). The constant values of Eq. (4) (A_D, n_D) are given in

Table 6 separately for mixtures of $C_{u,s}<5$ and $C_{u,s}>5$, whereas the constant values of Eq. (6) (A_6, A_7) are given in Table 7 as a function of the ratio $D_{50,s}/D_{50,r}$. In Eqs. (4)–(6), $DT_{O,mix}$, $DT_{O,mix,100}$, $DT_{soil,100}$ and pr are given in percentile scale (%), whereas σ'_m is given in kPa

$$DT_{O,mix} = DT_{O,mix,100} \times A_D \times (\sigma'_m)^{n_D} \quad (4)$$

$$DT_{O,mix,100} = DT_{O,soil,100} \times F(pr_d) \quad (5)$$

$$F(pr_d) = A_6 \times (pr) + A_7 \quad (6)$$

3.2. Synopsis of the experimental G/G_O and DT values versus the shearing strain amplitude

Fig. 3 presents the variation of G/G_O and DT with shear strain for the 'parent' granular soils (dry 71.1×142.2 mm specimens with 0% rubber content), while Fig. 4 presents the same for mixtures of sand/rubber (SRM) and gravel/rubber (GRM) (dry 71.1×142.2 mm^2 specimens of 5–35% rubber content by mixture weight), respectively. In the same figures we plot a spectrum of G/G_O–log γ–DT curves proposed by Menq [45] for clean sands and gravels. In accordance to Menq [45] the G/G_O–log γ–DT curves of granular soils become more linear with increasing confining pressure and decreasing coefficient of uniformity. The specimens of this study were tested in a range of σ'_m from 25 to 400 kPa. In addition, the parent soils exhibit a coefficient of uniformity from 1 to 13, approximately. Consequently, we decided to plot in Figs. 3 and 4 the following extreme curves; a curve of "linear" shape that corresponds to a uniform fine grained sand with $C_u=1$, $D_{50}=0.6$ mm at $\sigma'_m=400$ kPa, and a curve of "non-linear" shape that corresponds to a well-graded soil with $C_u=13$, $D_{50}=3.0$ mm at $\sigma'_m=25$ kPa.

Table 7
Parameters for the estimation of the function $F(pr_d)$.

No.	Mixture group	A_6	A_7
1	$D_{50,s} \ll D_{50,r}$	0.1004	1
2	$D_{50,s} \approx D_{50,r}$	0.1487	1
3	$D_{50,s} \gg D_{50,r}$	0.3683	1

The experimental values of the clean granular soils are in general within the upper and lower literature curves. The scatter of the G/G_O and DT values at specific shearing strain amplitude of Fig. 3 is mainly due to the effect of the confining pressure and the variation of grain size characteristics of the granular soils. Further analysis of the non-linear behavior of the granular soils used in this research may be found in [36,44].

The wide range spectrum of the experimental values for the SRM and GRM illustrated in Fig. 4 is the result of four important factors: the rubber content in the mixture, the confining pressure, the grain-size characteristics and dynamic properties of the physical portion of the mixtures, and the relative size of soil versus rubber particles expressed as $D_{50,s}/D_{50,r}$. It is shown that the addition of rubber in the soil results in a more linear behavior

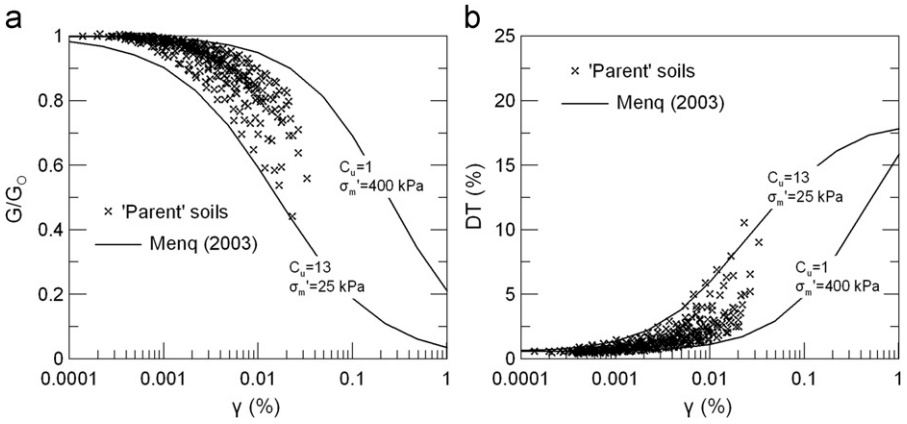

Fig. 3. Synopsis of the experimental (a) G/G_O–log γ and (b) DT–log γ values of the tested clean sandy and gravelly soils (in the same figure the proposed curves by Menq [45] for granular soils are also shown).

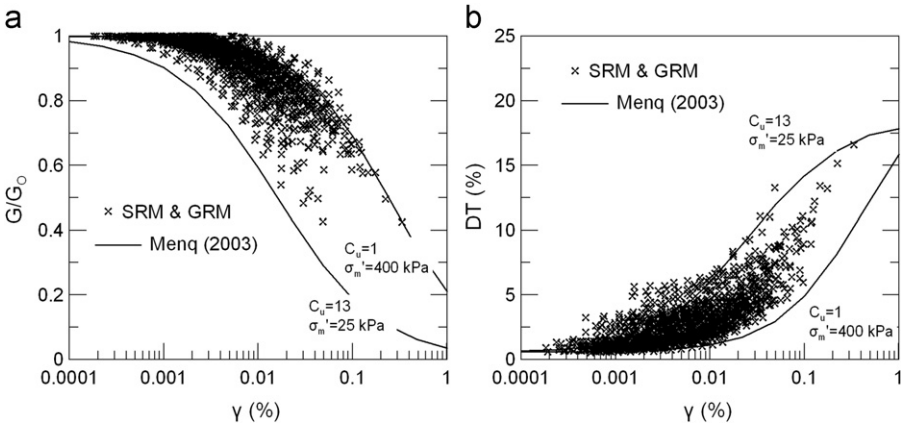

Fig. 4. Synopsis of the experimental (a) G/G_O–log γ and (b) DT–log γ values of the tested SRM and GRM (in the same figure the proposed curves by Menq [45] for granular soils are also shown).

with relatively higher damping. In the following we will further investigate the dynamic characteristics of the SRM and GRM.

3.3. Effect of shearing strain amplitude, confining pressure and rubber content on the non-linear shear modulus and damping ratio

In Figs. 5–7 we depict the effect of shearing strain amplitude (γ) and mean confining pressure (σ'_m) on the G/G_O and DT values of three specimens of mixture group C1D8-R2 (C1D8: fine gravel, R2: medium-grained rubber) having rubber contents equal to 0%, 15% and 25% by mixture weight. The results in these figures are representative of all mixture groups tested. In the same figures, the well-known spectrum of G/G_O–log γ–DT curves for sands proposed by Seed et al. [46] is also shown.

As expected the increase of shear strain amplitude (γ) reduces the shear modulus, and increases the damping. In addition, the increase of mean confining pressure (σ'_m) leads to more 'linear' behavior; at the same shear strain amplitude, G/G_O values increase whereas DT

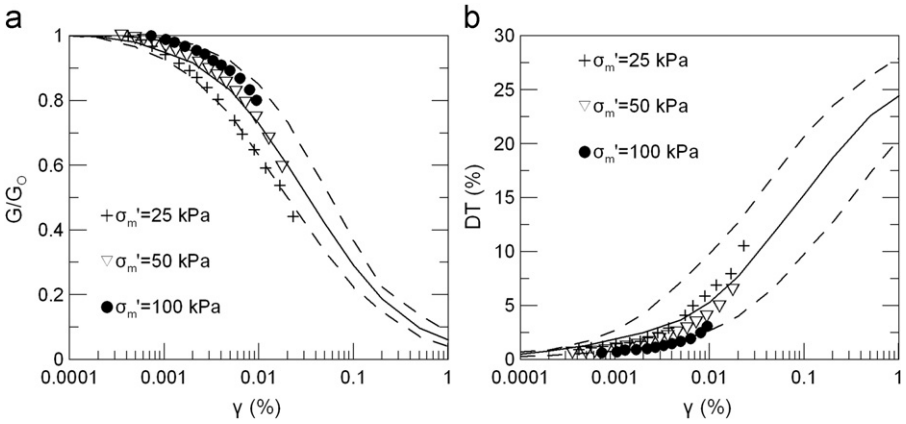

Fig. 5. Effect of shear strain amplitude, γ, and confining pressure, σ'_m, on (a) G/G_O and (b) DT of clean gravel C1D8 (in the same figure the proposed curves by Seed et al. [46] for sandy soils are also shown).

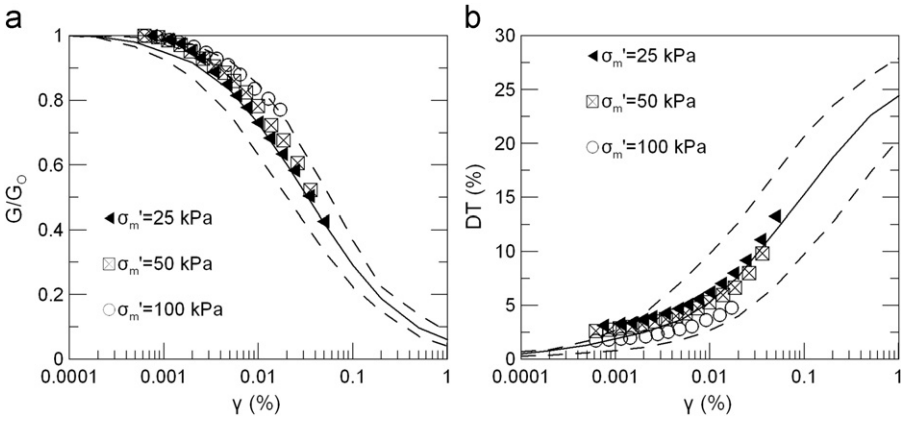

Fig. 6. Effect of shear strain amplitude, γ, and confining pressure, σ'_m, on (a) G/G_O and (b) DT of GRM C1D8-R2-85/15 having 15% rubber by mixture weight (in the same figure the proposed curves by Seed et al. [46] for sandy soils are also shown).

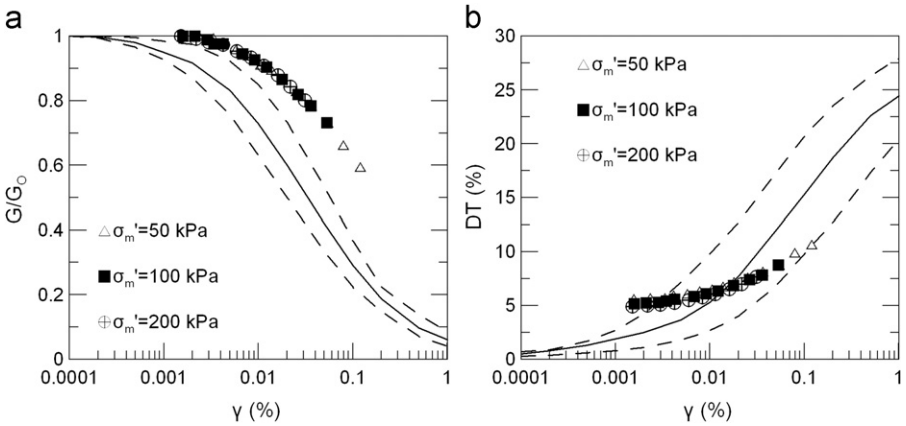

Fig. 7. Effect of shear strain amplitude, γ, and confining pressure, σ'_m, on (a) G/G_O and (b) DT of GRM C1D8-R2-75/25 having 25% rubber by mixture weight (in the same figure the proposed curves by Seed et al. [46] for sandy soils are also shown).

values slightly decrease as σ'_m increases. This observation is more pronounced in the case of specimens C1D8 and C1D8-R2-85/15 (Figs. 5 and 6). In general it is shown that the effect of shear strain amplitude and confining pressure (σ'_m) on the cyclic response of soil/rubber mixtures follows a similar trend as for clean granular soils.

In Figs. 8–10 we present the effect of rubber content on the G/G_O–log γ–DT curves of representative SRM and GRM. DT values are normalized herein with respect to the corresponding damping ratio values at small strain level, in terms of DT–DT_O, in order to eliminate the effect of DT_O on the experimental results. Figs. 8 and 9 concern the mixture groups C1D8-R2 and C6D3-R3 at $\sigma'_m = 100$ kPa, whereas Fig. 10 concerns the mixture group C2D03-R03 at $\sigma'_m = 50$ kPa. In agreement to previous studies [29,33–35] the increase of rubber content leads to more linear shape of the G/G_O–log γ–DT curves; this is more pronounced for rubber content equal to or higher than 15%, by mixture weight.

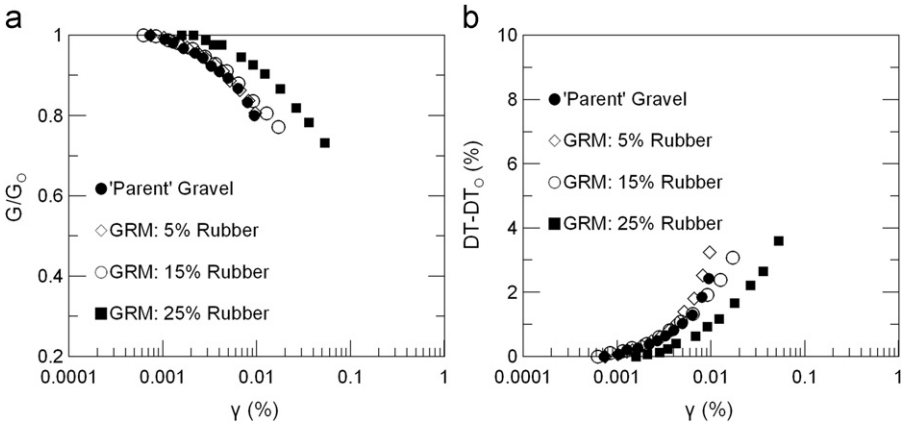

Fig. 8. Effect of rubber content on (a) G/G_O–log γ and (b) DT–log γ curves of mixture group C1D8-R2 at $\sigma'_m = 100$ kPa (DT values are normalized with respect to the corresponding small-strain damping ratio in terms of DT–DT_O).

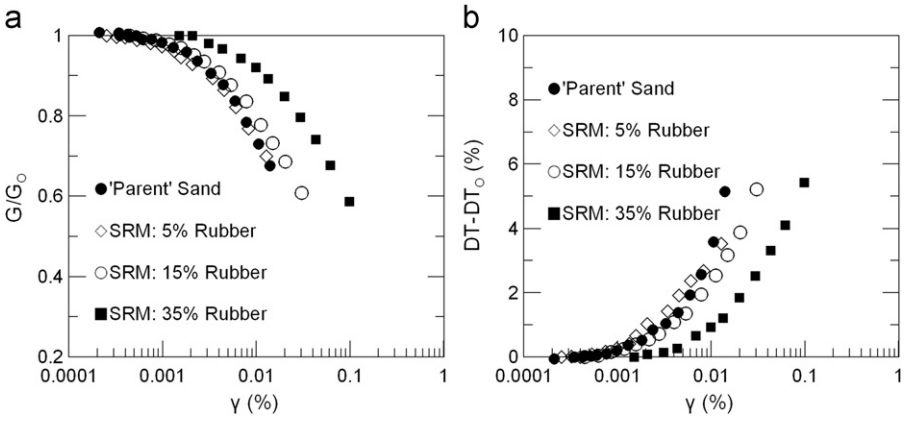

Fig. 9. Effect of rubber content on (a) G/G_O–log γ and (b) DT–log γ curves of mixture group C6D3-R3 at $\sigma'_m = 100$ kPa (DT values are normalized with respect to the corresponding small-strain damping ratio in terms of DT–DT_O).

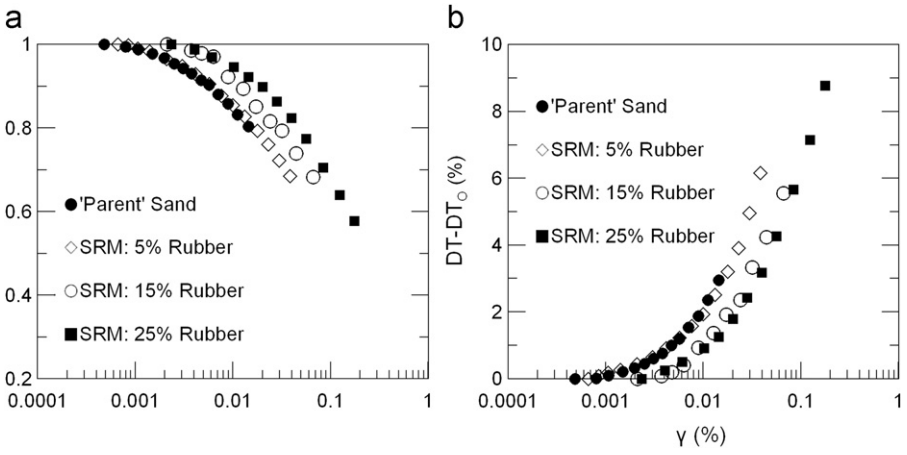

Fig. 10. Effect of rubber content on (a) G/G_O–log γ and (b) DT–log γ curves of mixture group C2D03-R03 at $\sigma'_m = 50$ kPa (DT values are normalized with respect to the corresponding small-strain damping ratio in terms of DT–DT_O).

3.4. Generic normalized shear modulus versus shearing strain curves

3.4.1. Analytical model

The effect of rubber inclusion and content on the normalized shear modulus values is studied herein utilizing the modified hyperbolic model [47–49]. The variation of G/G_O with shear strain is expressed by Eq. (7) having two fitting parameters; the reference strain (γ_{ref}) and the curvature coefficient (a). Reference strain is the shear strain amplitude for $G/G_O=0.5$, and expresses the linearity of the G/G_O–$\log\gamma$ curve, whereas parameter (a) expresses the overall slope of the G/G_O–$\log\gamma$ curve [45,48,49]

$$\frac{G}{G_O}=\frac{1}{1+(\gamma/\gamma_{ref})^a} \tag{7}$$

Fig. 11 depicts a representative example of the implementation of the modified hyperbolic model on the measured G/G_O values of the mixture group C2D3-R06 for rubber contents equal to 15% and 25% (specimens C2D3-R06-85/15 and C2D3-R06-75/25 respectively) at $\sigma'_m=50$ kPa. Specimen C2D3-R06-85/15 exhibits values of the fitting parameters equal to $\gamma_{ref}=4.2\times10^{-2}$% and $a=0.87$, whereas specimen C2D3-R06-75/25 exhibits values $\gamma_{ref}=1.2\times10^{-1}$% and $a=0.81$. Thus, the more linear behavior of the SRM and GRM with increasing the content of rubber may be correlated to the increasing reference strain values.

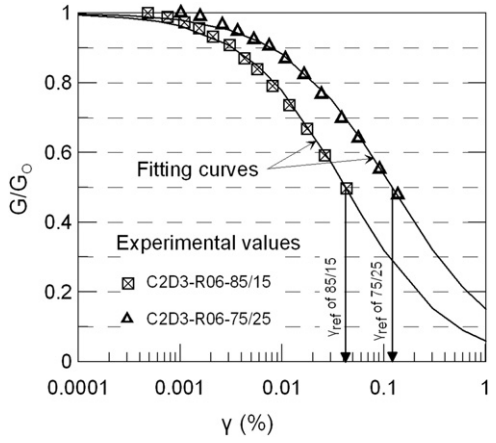

Fig. 11. Implementation of the modified hyperbolic model on the experimental G/G_O values versus the shear strain amplitude: specimens of mixture group C2D3-R06 having rubber contents equal to 15% and 25% by mixture weight at $\sigma'_m=50$ kPa.

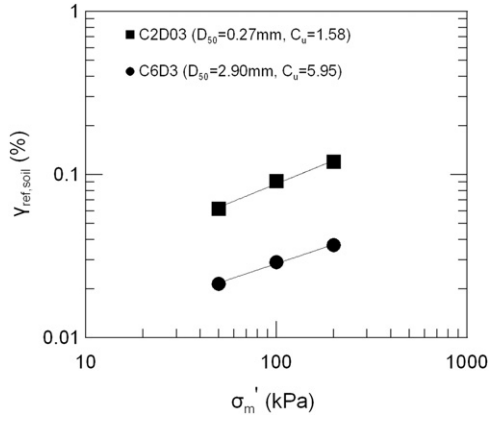

Fig. 12. Effect of mean confining pressure, σ'_m, on reference strain, $\gamma_{ref,soil}$, of clean granular soils of variable grain-size characteristics.

3.4.2. Reference strain of SRM and GRM at $\sigma'_m=100$ kPa

In Fig. 12 we plot the reference strain values symbolized as $\gamma_{ref,soil}$ versus σ'_m of two clean soils of this study; specimen C2D03 is a uniform fine-grained sand with $C_u=1.58$ and $D_{50}=0.27$ mm, while specimen C6D3 is a well-graded gravelly sand with $C_u=5.95$ and $D_{50}=2.95$ mm. The increase of σ'_m leads to higher $\gamma_{ref,soil}$ values in both specimens, whereas the well-graded gravelly sand exhibits significantly lower $\gamma_{ref,soil}$ values, that is more pronounced nonlinearity in the region of medium to high strains, in comparison to the uniform fine-grained sand. The effect of grain-size characteristics on the G/G_O–$\log\gamma$–DT curves of the clean granular soils tested herein is thoroughly discussed by Anastasiadis et al. [44] and Senetakis [36].

Fig. 13 illustrates the effect of rubber content on the reference strain of mixture groups C2D03-R3 and C6D3-R3 at $\sigma'_m=100$ kPa, symbolized as $\gamma_{ref,mix,100}$. According to these results the reference strain $\gamma_{ref,mix,100}$ of both mixture groups increases as rubber content increases, while the mixture group C6D3-R3 exhibits systematically lower $\gamma_{ref,mix,100}$ values compared to mixture group C2D03-R3. The first observation is in accordance to the results of Figs. 8–11 and thus, the more linear shape of the G/G_O–$\log\gamma$ curves of mixtures with increasing rubber content, is reacted to the increase of reference strain. The second observation indicates that the response of the mixtures in the region of medium to high shear strains and for the rubber contents used herein (0–35% by mixture weight) is significantly controlled by the natural-soil portion of the mixtures; the lower reference strain values of mixture group C6D3-R3 compared to mixture group C2D03-R3, are mainly due to the lower reference strain values of the 'parent' soil C6D3 compared to the 'parent' soil C2D03 as depicted in Fig. 12.

Thus, the reference strain of the SRM and GRM at a mean confining pressure of 100 kPa may be expressed with the following analytical expression:

$$\gamma_{ref,mix,100}=\gamma_{ref,soil,100}\times F(pr_\gamma) \tag{8}$$

where $\gamma_{ref,mix,100}$ and $\gamma_{ref,soil,100}$ is the reference strain at $\sigma'_m=100$ kPa of the SRM (or GRM) and the 'parent' soil, respectively, and $F(pr_\gamma)$ is a function that expresses the effect of rubber content (pr) on mixtures' reference strain, given from the following equation:

$$F(pr_\gamma)=a_1\times(pr)^2+a_2\times(pr)+a_3 \tag{9}$$

where a_1, a_2 and a_3 are constants.

In Fig. 14 we show the effect of the content of rubber (pr) and the relative size of soil grains versus rubber solids ($D_{50,s}/D_{50,r}$) on mixtures' reference strain at $\sigma'_m=100$ kPa. Reference strain values

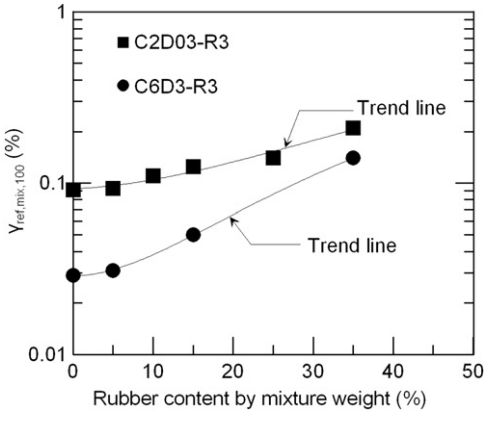

Fig. 13. Effect of the content of rubber and the natural-soil portion of SRM and GRM on the reference strain values: Experimental results of mixture groups C2D03-R3 and C6D3-R3 at $\sigma'_m=100$ kPa.

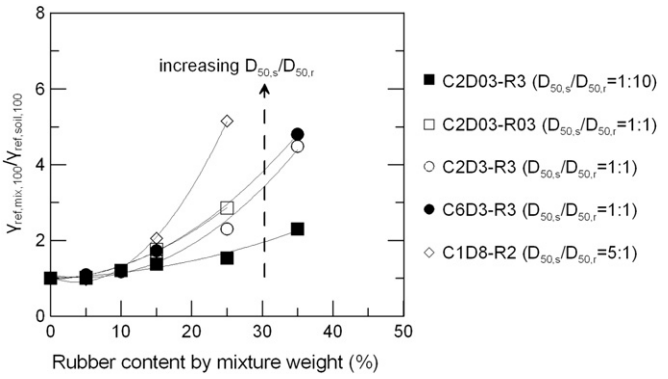

Fig. 14. Effect of the content of rubber and the relative size of soil versus rubber particles expressed as $D_{50,s}/D_{50,r}$ on the reference strain of SRM and GRM.

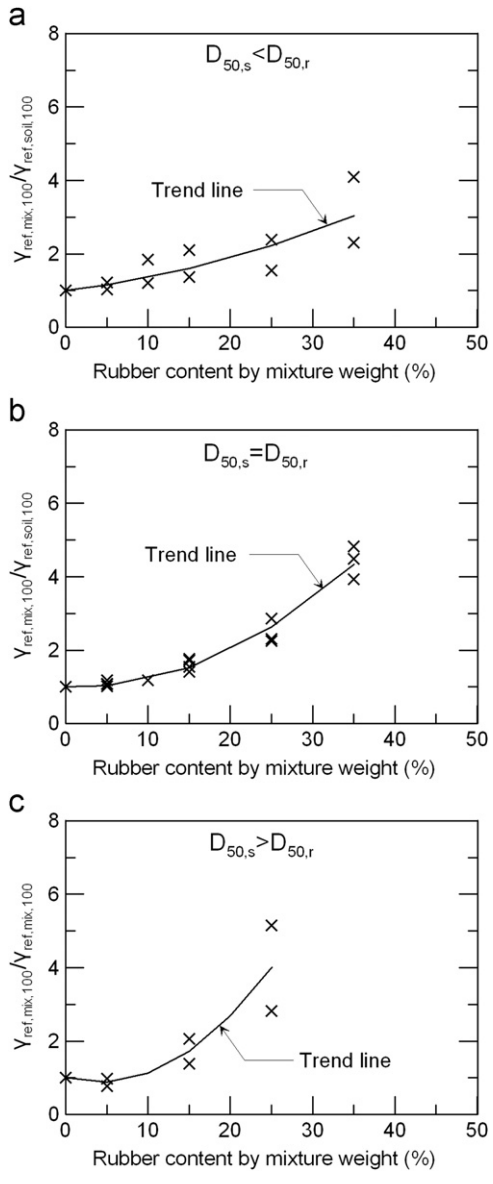

Fig. 15. Effect of the content of rubber on the ratio $\gamma_{ref,mix,100}/\gamma_{ref,soil,100}$ for SRM and GRM of variable $D_{50,s}/D_{50,r}$ ratios.

of the mixtures are normalized herein with respect to the corresponding values of the intact soils at the same confining pressure ($\gamma_{ref,mix100}/\gamma_{ref,soil,100}$). For low to medium rubber contents

Table 8
Proposed constant values for the estimation of the $F(pr_\gamma)$ function of the SRM and GRM and corresponding correlation coefficient values R^2.

No.	Mixture category	a_1	a_2	a_3	R^2
1	$D_{50,s}$[a] < $D_{50,r}$[b]	0.0009	0.0266	1.00	0.69
2	$D_{50,s}=D_{50,r}$	0.0030	−0.0100	1.00	0.97
3	$D_{50,s}>D_{50,r}$	0.0072	−0.0599	1.00	0.81

[a] Mean grain size of soil particles of SRM and GRM.
[b] Mean grain size of rubber particles of SRM and GRM.

($pr \leq 15\%$) all mixture groups follow a similar trend of increasing the ratio ($\gamma_{ref,mix100}/\gamma_{ref,soil,100}$); the inclusion of rubber solids leads to more flexible specimens and thus to more linear response in the region of medium to high strains. However, the overall response of the SRM and GRM solid matrix is mainly controlled by the soil portion. For rubber contents above 15%, the increase of reference strain is a function of both the content of rubber and the ratio $D_{50,s}/D_{50,r}$.

In the region of medium to high rubber contents ($15\% \leq pr \leq 35\%$ by weight), mixtures transform gradually from sand-like to rubber-like behavior due to the development of rubber-to-rubber interfaces; for rubber contents above 35% by mixture weight (or about 55–60% by mixture volume) the response of the mixtures is controlled by the rubber part of the soil/rubber solid matrix [20]. However, Kim and Santamarina [20] concluded that the transformation from sand-like to rubber-like behavior is observed for lower rubber contents as the ratio $D_{50,s}/D_{50,r}$ increases. Practically, at the same content of rubber above 15% by mixture weight, the increase of the ratio $D_{50,s}/D_{50,r}$ increases the rubber-to-rubber interfaces and consequently the ratio ($\gamma_{ref,mix100}/\gamma_{ref,soil,100}$) increases in a more pronounced way as shown in Fig. 14.

In Fig. 15a–c we plot the reference strain values at $\sigma'_m = 100$ kPa of all SRM and GRM specimens with the content of rubber. The reference strain is normalized with respect to the corresponding reference strain of the 'parent' soils, in terms of the ratio $\gamma_{ref,mix100}/\gamma_{ref,soil,100}$. In addition, mixtures are separated in three categories with respect to the ratio $D_{50,s}/D_{50,r}$. In the same figures we show graphically the increasing reference strain with increasing rubber content. The increasing trend lines are expressed analytically by the function $F(pr_\gamma)$ of Eqs. (8) and (9). The estimated values of the constants a_1, a_2 and a_3 as well as the correlation coefficients (R^2) of the mixtures are summarized in Table 8, separately for mixtures of $D_{50,s} < D_{50,r}$, $D_{50,s} = D_{50,r}$ and $D_{50,s} > D_{50,r}$.

To conclude, the reference strain of a granular soil/rubber mixture at $\sigma'_m = 100$ kPa may be determined from Eqs. (8) and (9) and the constant values of Table 8. For this it is necessary to know the appropriate values of the reference strain of the clean granular soil at $\sigma'_m = 100$ kPa, the content of rubber in the mixture expressed by mixture weight, and the ratio of mean grain size of soil versus rubber solids, $D_{50,s}/D_{50,r}$.

The parameters $\gamma_{ref,mix100}$, $\gamma_{ref,soil,100}$ and pr of Eqs. (8) and (9) are given in percentile scale (%), whereas parameter $\gamma_{ref,soil,100}$ is a function of the grain size characteristics of the soil. For sandy and gravelly materials, proposed equations for the estimation of reference strain are given in [36,44].

3.4.3. Reference strain of SRM and GRM as a function of σ'_m

The effect of mean confining pressure on the reference strain of the SRM and GRM, symbolized as $\gamma_{ref,mix}$, may be analytically expressed with the general form of Eq. (10):

$$\gamma_{ref,mix} = \gamma_{ref,mix,100} \times A_{\gamma,mix} \times (\sigma'_m)^{n_{\gamma,mix}} \quad (10)$$

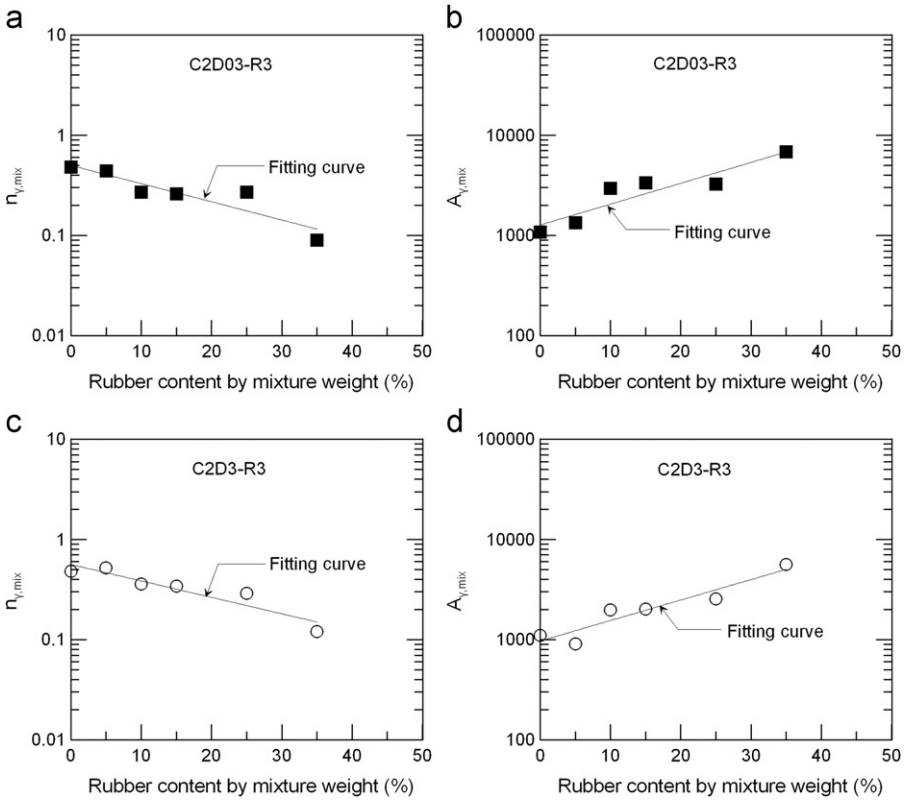

Fig. 16. Effect of rubber content on the parameters $n_{\gamma,mix}$ and $A_{\gamma,mix}$ of (a, b) mixture group C2D03-R3 and (c, d) mixture group C2D3-R3.

where $\gamma_{ref,mix,100}$ is the reference strain of the SRM and GRM at $\sigma'_m = 100$ kPa, $A_{\gamma,mix}$ is a parameter of the statistical (regression) analysis and $n_{\gamma,mix}$ is an exponent that expresses the slope of the diagram $\gamma_{ref,mix} - \sigma'_m$ in log scale.

In Fig. 16, the effect of rubber content on the parameters $n_{\gamma,mix}$ and $A_{\gamma,mix}$ of mixture groups C2D03-R3 and C2D3-R3 is depicted in semi-log plots. There is a general trend of decreasing $n_{\gamma,mix}$ and increasing $A_{\gamma,mix}$ as rubber content increases. The decrease of $n_{\gamma,mix}$ indicates that the effect of confining pressure on the G/G_O–log γ–DT curves becomes less pronounced for higher rubber contents, while the increase of $A_{\gamma,mix}$ indicates that reference strain increases with the increase of rubber content and thus, G/G_O–log γ–DT curves exhibit more linear shape.

In Fig. 17 we show the effect of rubber content on the parameters $n_{\gamma,mix}$ and $A_{\gamma,mix}$ of all the SRM and GRM under this study. Parameters $n_{\gamma,mix}$ and $A_{\gamma,mix}$ are normalized herein with respect to the corresponding values of the 'parent' soils, symbolized as $n_{\gamma,soil}$ and $A_{\gamma,soil}$. In the same figures the trend lines of decreasing $n_{\gamma,mix}$ and increasing $A_{\gamma,mix}$ with rubber content are also shown. We underline that there was not observed a clear trend of the effect of $D_{50,s}/D_{50,r}$ ratio on the parameters $n_{\gamma,mix}$ and $A_{\gamma,mix}$ and thus, mixtures are not separated in Fig. 17 in sub-categories.

It should be noticed that the scatter of the experimental data in Fig. 17 is not insignificant. However, as will be discussed later in this paper, the overall prediction of the strain-dependent dynamic properties of the SRM/GRM using the analytical equations proposed on the framework of this study is satisfactory and acceptable for geotechnical engineering purposes.

The aforementioned scatter of the experimental data is possibly related to the fact that parameters $n_{\gamma,mix}$ and $A_{\gamma,mix}$ were derived through regression analysis by plotting the reference strain versus the mean confining pressure for each specimen, where the reference strain values were determined through the

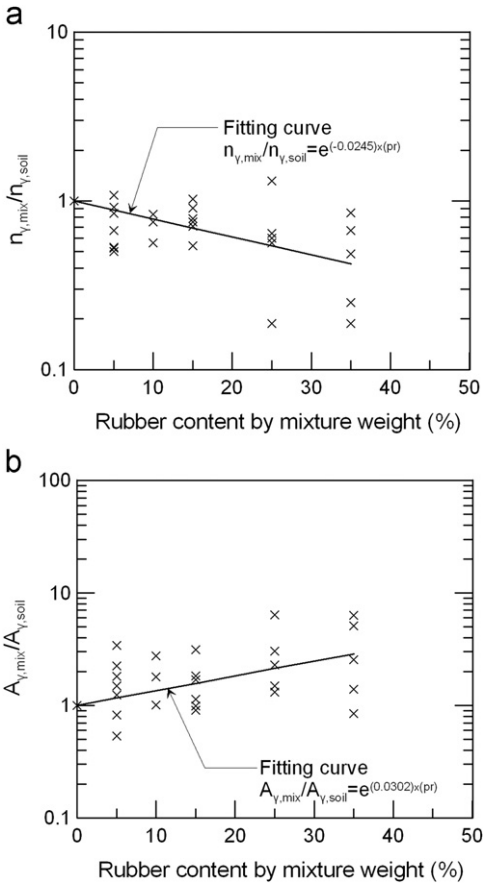

Fig. 17. Normalized parameters $n_{\gamma,mix}/n_{\gamma,soil}$ and $A_{\gamma,mix}/A_{\gamma,soil}$ versus rubber content of all SRM and GRM under this study.

modified hyperbolic model. In other words, these parameters are not derived "experimentally" but "theoritically" and at the same time parameters $n_{\gamma,mix}$ and $A_{\gamma,mix}$ (expressed in this study in terms of the ratios $n_{\gamma,mix}/n_{\gamma,soil}$ and $A_{\gamma,mix}/A_{\gamma,soil}$) are sensitive to small changes in reference strain values (which is also the case in clean granular soils [36]) and thus this sensitivity introduces some scatter on the experimental data of Fig. 17.

Furthermore, the scatter of the experimental data of Fig. 17 is also related to the fact that we performed tests on mixtures that are composed of soils of variable grain-size distribution and particles' shape, the ratio $D_{50,s}/D_{50,r}$ ranges between 1:10 and 5:1 and overall, the inclusion of rubber particles in the mixtures adds more complexity to the resultant response of the specimens.

The regression analysis of the experimental results led to the Eqs. (11a) and (11b) for the estimation of the parameters $n_{\gamma,mix}$ and $A_{\gamma,mix}$ as a function of the corresponding parameters of the 'parent' soils and the content of rubber (pr in percentile scale)

$$n_{\gamma,mix} = n_{\gamma,soil} \times e^{a_4 \times (pr)} \tag{11a}$$

$$A_{\gamma,mix} = A_{\gamma,soil} \times e^{a_5 \times (pr)} \tag{11b}$$

Table 9 summarizes the $n_{\gamma,soil}$ and $A_{\gamma,soil}$ values of the seven clean sandy and gravelly specimens, as well as the average values of these parameters. Finally, in Fig. 17 we depict the values of a_4 and a_5, estimated as -0.0245 and 0.0302, respectively. Consequently, Eqs. (11a) and (11b) may be transformed to Eqs. (12a) and (12b).

$$n_{\gamma,mix} = 0.40 \times e^{-0.0245 \times (pr)} \tag{12a}$$

$$A_{\gamma,mix} = 0.1771 \times e^{0.0302 \times (pr)} \tag{12b}$$

To conclude, given the content of rubber by mixture weight (pr), and the mean confining pressure (σ'_m), the reference strain of a granular soil/rubber mixture may be estimated from Eqs. (10), (12a) and (12b), where the parameter $\gamma_{ref,mix,100}$ is given in the previous paragraph. The reference strain of equation (10) and the content of rubber of Eqs. (12a) and (12b) are given in percentile scale (%), whereas the mean confining pressure, σ'_m, of Eq. (10) is given in kPa.

3.4.4. Curvature coefficient of SRM and GRM

Fig. 18 depicts the curvature coefficient values (a), of all specimens, with the rubber content. No clear effect of confining pressure (σ'_m) or rubber content (pr) on curvature coefficient (a) has been observed and thus it was decided to determine an average curvature coefficient value, also shown in Fig. 18. Representative a–σ'_m diagrams for variable rubber contents were presented by Senetakis et al. [35] and Senetakis [36], whereas the effect of specimens geometry on curvature coefficient (a) is further discussed by Senetakis et al. [34].

Table 9
Average $n_{\gamma,soil}$ and $A_{\gamma,soil}$ of the 'parent' granular soils.

No.	'Parent' soil	$n_{\gamma,soil}$	$A_{\gamma,soil}$
1	C2D03	0.48	0.1076
2	C3D06	0.42	0.1940
3	C2D1	0.29	0.2871
4	C2D3	0.48	0.1106
5	C6D3	0.39	0.1617
6	C13D3	0.34	0.2122
7	C1D8	0.39	0.1667
8	Average value	0.40	0.1771
9	Standard deviation	0.07	0.0622

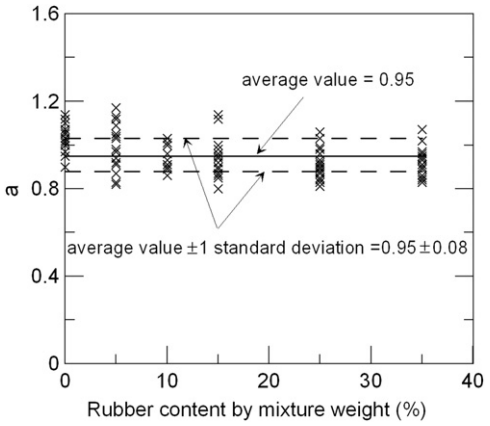

Fig. 18. Curvature coefficient, a, versus rubber content, pr, of all SRM and GRM (dry 71.1 × 142.2 mm specimens, rubber content from 0% to 35%, confining pressure from 25 to 400 kPa).

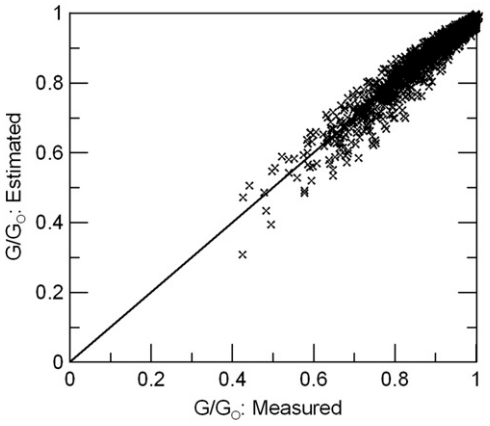

Fig. 19. Measured versus estimated normalized shear modulus values of SRM and GRM.

3.4.5. Comparison between measured and analytically derived normalized shear modulus

The hyperbolic model of Eq. (7) may be further modified for the SRM and GRM of this study to Eq. (13). Then, G/G_O values of a granular soil/rubber mixture may be estimated as a function of the shear strain amplitude (γ) from Eqs. (9) to (13) and the constants given in Tables 8 and 9

$$\frac{G}{G_O} = \frac{1}{1+(\gamma/\gamma_{ref})^{0.95}} \tag{13}$$

The measured versus the analytically derived normalized shear modulus values are plotted in Fig. 19. The reference strain values of the clean granular soils, $\gamma_{ref,soil,100}$, of Eq. (8) were estimated herein using the analytical equations proposed by Anastasiadis et al. [44] and Senetakis [36]. The comparison is quite satisfactory. The correlation coefficient (R^2) between the measured and the analytically derived values is equal to 0.97.

3.5. Generic damping ratio versus shearing strain curves

As discussed in [33–36,38] the DT–$\log\gamma$ curves of SRM and GRM may be studied in terms of G/G_O versus DT–DT_O values, where DT_O is the small-strain damping ratio.

Fig. 20 depicts representative results for the mixture group C2D03-R3 at $\sigma'_m = 100$ kPa and rubber contents equal to 0%, 10% and 25%. In particular in Fig. 20a the damping DT values are

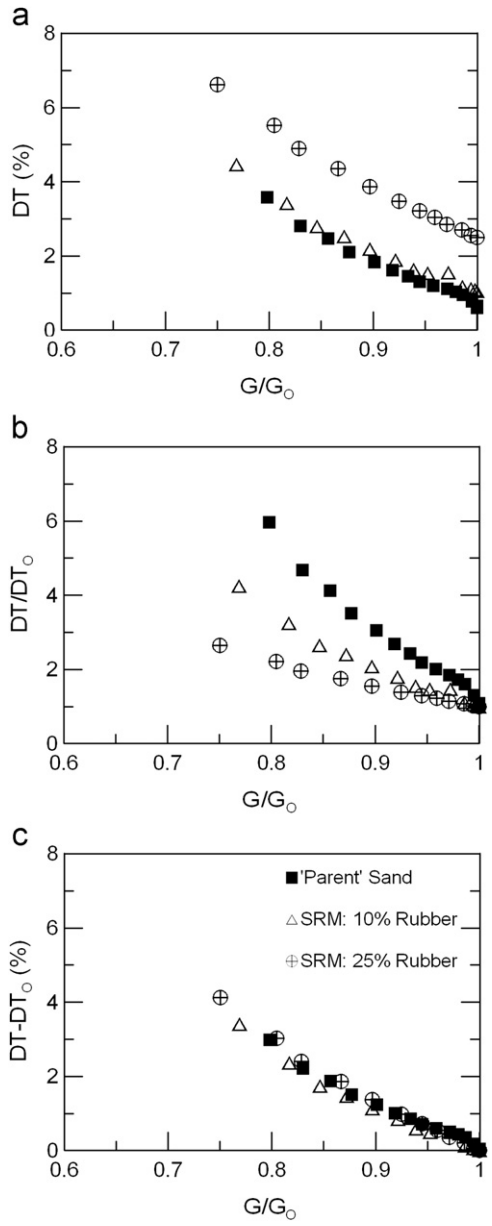

Fig. 20. Normalized shear modulus, G/G_O, versus (a) damping ratio, DT, (b) normalized damping ratio in terms of DT/DT_O, and (c) normalized damping ratio in terms of $DT–DT_O$ of mixture group C2D03-R3 at $\sigma'_m = 100$ kPa.

plotted against the corresponding G/G_O values, while the G/G_O values are plotted against the DT/DT_O and $DT–DT_O$ values in Fig. 20b and c, respectively. The plot of DT versus G/G_O (Fig. 20a) includes the effect of DT_O and thus the effect of rubber content on the experimental results. This is also the case of Fig. 20b, where we notice that the normalization of damping ratio values in terms of DT/DT_O involves the effect of rubber inclusion; specimens of higher rubber content exhibit more linear shape of the DT/DT_O versus G/G_O curves. On the contrary, the normalization of damping ratio in terms of $DT–DT_O$ (Fig. 20c) eliminates the effect small-strain damping ratio and thus, the effect of rubber content on the experimental results.

In Fig. 21 we plot the $DT–DT_O$ values versus G/G_O of all SRM and GRM specimens of this study with rubber content varying from 0% to 35% by mixture weight, and σ'_m varying from 25 to 400 kPa. In the same figure we illustrate the fitting curve of the experimental results. In that way we may estimate the normalized damping ratio, $DT–DT_O$, of SRM and GRM, as a function of the

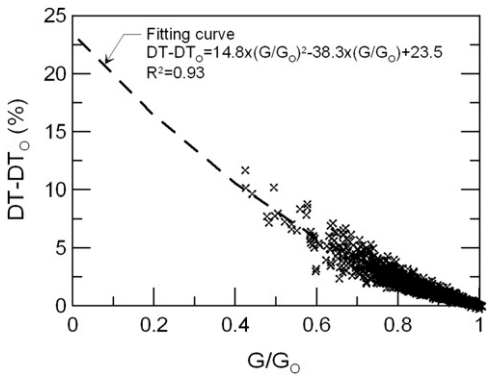

Fig. 21. Correlation between $DT–DT_O$ and G/G_O of SRM and GRM.

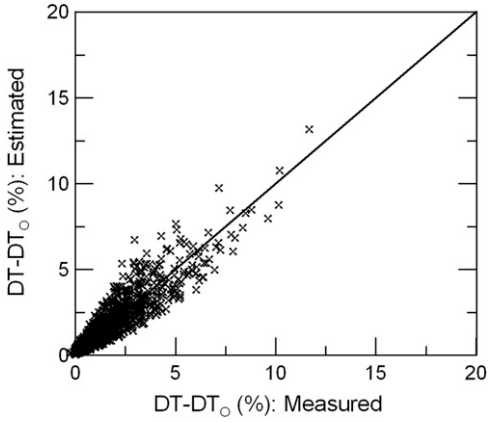

Fig. 22. Measured versus estimated normalized damping ratio values of SRM and GRM.

corresponding G/G_O, from Eq. (14). Then, damping ratio, DT, may be estimated as a function of DT_O (see Section 3.1)

$$DT-DT_O(\%) = a_6 \times \left(\frac{G}{G_O}\right)^2 + a_7 \times \left(\frac{G}{G_O}\right) + a_8 \quad (14)$$

where $a_6 = 14.8$, $a_7 = -38.3$ and $a_8 = 23.5$.

Finally, in Fig. 22 we plot the measured versus the analytically derived $DT–DT_O$ values. Normalized damping ratio values are estimated using Eq. (14), whereas the G/G_O values of this equation are estimated using the proposed relationships presented in Section 3.4. The correlation coefficient (R^2) between the measured and the analytically derived $DT–DT_O$ values is equal to 0.93.

3.6. Design G/G_O–log γ and DT–log γ curves for granular soil/rubber mixtures

Using the equations presented previously, in Figs. 23 and 24 we propose a set of G/G_O–log γ and DT–log γ curves for SRM and GRM materials, respectively, for variable rubber contents and confining pressures. The design curves are parameterized with the following parameters: Concerning Fig. 23 (SRM), $D_{50,s} = 0.60$ mm, $C_{u,s} < 5$, $D_{50,s} < D_{50,r}$, $\gamma_{ref,soil,100} = 4.22 \times 10^{-2}$%, $DT_{O,soil,100} = 0.63$%, whereas concerning Fig. 24 (GRM), $D_{50,s} = 3.00$ mm, $C_{u,s} > 5$, $D_{50,s} = D_{50,r}$, $\gamma_{ref,soil,100} = 2.97 \times 10^{-2}$%, $DT_{O,soil,100} = 0.71$%. Parameters $\gamma_{ref,soil,100}$, $DT_{O,soil,100}$ (reference strain and small-strain damping ratio at $\sigma'_m = 100$ kPa of the intact soils, respectively) were determined using the analytical equations presented by Anastasiadis et al. [44] and Senetakis [36].

Fig. 25 presents the design G/G_O–log γ and DT–log γ curves at $\sigma'_m = 100$ kPa for GRM for variable rubber contents, using the

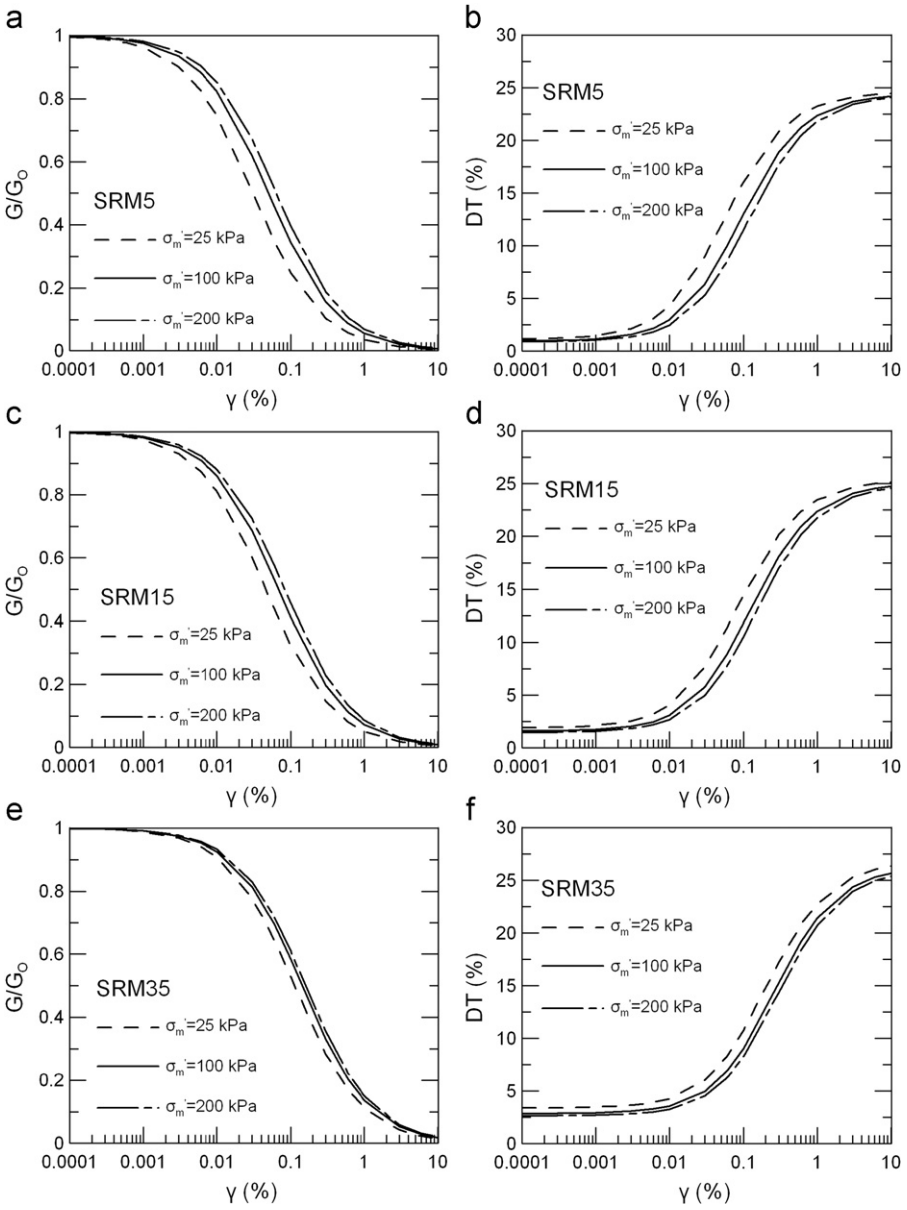

Fig. 23. Design G/G_O–log γ–DT curves for SRM for variable mean confining pressures (SRM5: 5% rubber my mixture weight, $D_{50,s} < D_{50,r}$).

parameters mentioned previously. It is shown that the increase in rubber content leads to higher G/G_O at the same σ'_m. However, for shear strain amplitudes above 10^{-2}% the increase of rubber content leads to lower DT values; this is due to the more linear shape of the DT–log γ curves with increasing rubber content.

Finally, in Fig. 26 we depict the effect of the relative size of soil versus rubber solids, expressed as $D_{50,r}/D_{50,s}$, on the G/G_O–log γ and DT–log γ curves of GRM25 materials considering 25% rubber by mixture weight and $\sigma'_m = 100$ kPa. As shown in Fig. 26a, the increase of the ratio $D_{50,s}/D_{50,r}$ leads to more linear G/G_O–log γ curves due to the more pronounced increase of rubber-to-rubber interfaces. It is also observed in Fig. 26b that the ratio $D_{50,s}/D_{50,r}$ significantly affects the DT–log γ curves.

It is concluded that for the accurate estimation of the non-linear response of granular soil/rubber mixtures, and thus, for the accurate seismic design of a structure or geo-structure where SRM or GRM is used, it is important to account the effect of the following main parameters: the content of rubber, the confining pressure and the relative size of soil versus rubber solids.

4. Conclusions and recommendations

In this paper we synthesized past and new high-amplitude resonant column tests in order to investigate the dynamic properties of granular soil/rubber mixtures and to propose generic and design shear modulus reduction and damping increase curves with increasing shear strain. In addition, we summarized analytical expressions for the estimation of the small-strain shear modulus and damping ratio of soil/rubber mixtures (SRM) and gravel/rubber mixtures (GRM) proposed in previous studies. The main conclusions of this comprehensive research are the following:

– The small-strain shear modulus ($G_{O,mix}$) and damping ratio ($DT_{O,mix}$) of the SRM and GRM are affected by the confining pressure (σ'_m), the content of rubber (pr), the grain-size characteristics and dynamic properties of the intact soils (having 0% rubber) and the relative size of soil versus rubber particles expressed as $D_{50,s}/D_{50,r}$. In general, $G_{O,mix}$ increases

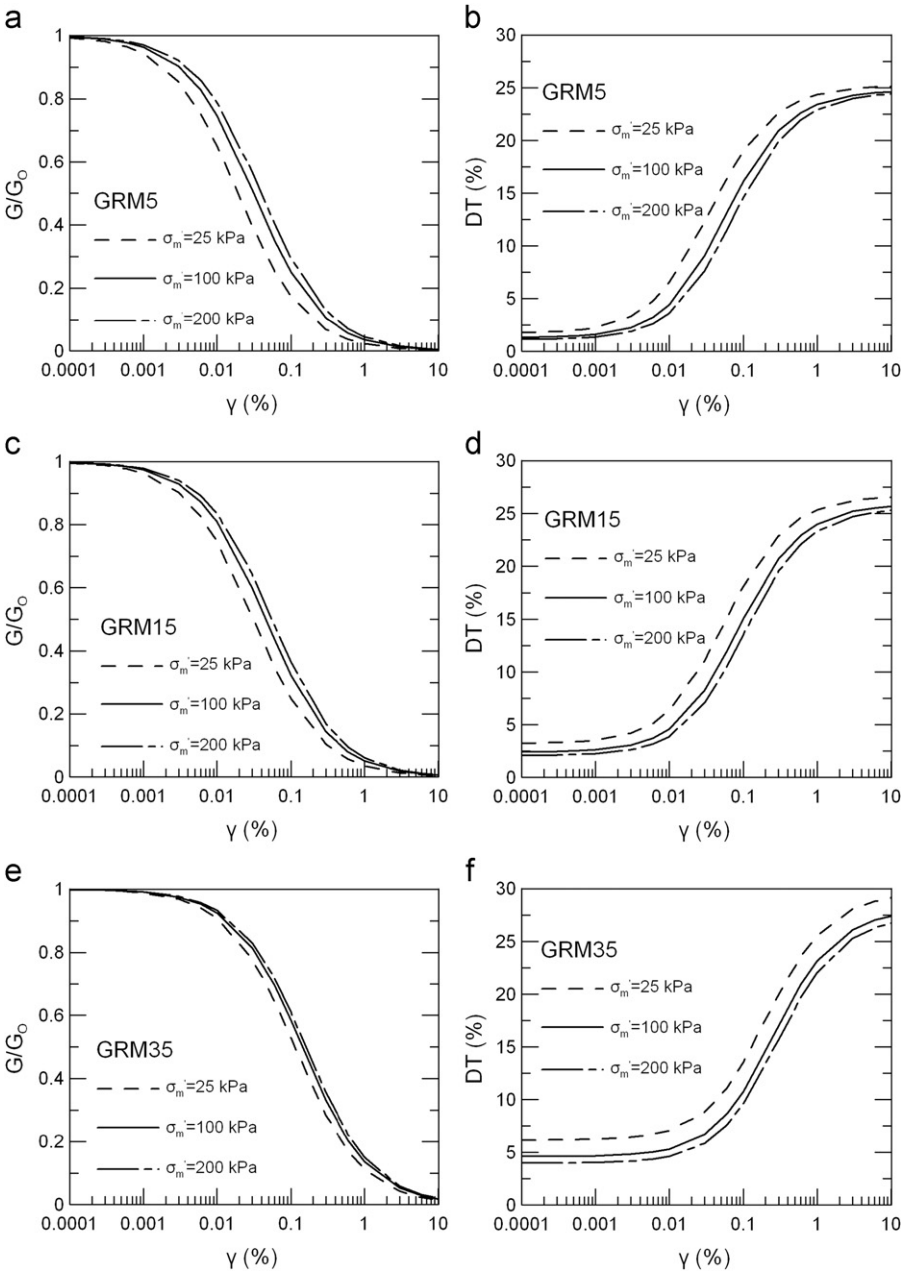

Fig. 24. Design G/G_O–log γ–DT curves for GRM for variable mean confining pressures (GRM5: 5% rubber my mixture weight, $D_{50,s}=D_{50,r}$).

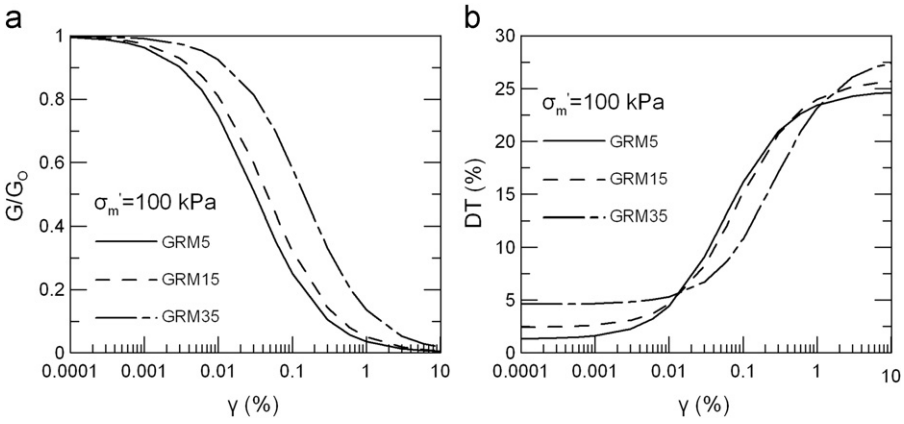

Fig. 25. Design G/G_O–log γ–DT curves for GRM at $\sigma'_m=100$ kPa for variable rubber contents (GRM5: 5% rubber my mixture weight, $D_{50,s}=D_{50,r}$).

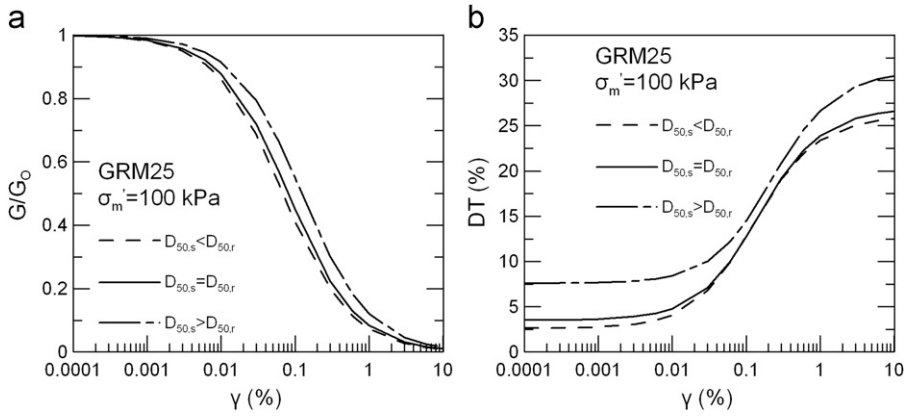

Fig. 26. Design G/G_O–log γ–DT curves for GRM at $\sigma'_m = 100$ kPa for variable $D_{50,s}/D_{50,r}$ ratios (GRM25: 25% rubber my mixture weight).

with increasing σ'_m and decreasing the content of rubber, whereas the opposite trend is observed for $DT_{O,mix}$. $G_{O,mix}$ is expressed in terms of an equivalent void ratio in which the volume of rubber particles is assumed to be part of the total volume of voids.

- SRM and GRM and concerning the range of rubber content used, between 0% and 35% by mixture weight, exhibit strain-dependent behavior, whereas, as in clean granular soils, the increase of confining pressure (σ'_m) leads to more linear shape of the G/G_O–log γ–DT curves. However, the increase of rubber content decreases the effect of σ'_m on the G/G_O–log γ–DT curves of the SRM and GRM.
- One major parameter that affects the non-linear response of the SRM and GRM is the content of rubber (pr). The increase of (pr) leads to more linear G/G_O–log γ–DT curves. This effect may be analytically studied by the increase of the reference strain of the mixtures with increasing rubber content.
- Mixtures composed of fine-grained uniform sands as physical portion exhibit higher values of reference strain and thus more linear shape of the G/G_O–log γ–DT curves in comparison to mixtures composed of gravelly, well-graded soils. This is due the higher 'linearity' that the fine-grained uniform sands exhibit in comparison to the gravelly soils. Consequently, the analysis of the results should include the effect of the physical portion of the mixtures in terms of grain-size characteristics.
- The increase of rubber content in the mixtures increases the rubber-to-rubber interfaces and thus mixtures gradually transform from sand-like to rubber-like behavior. At relatively high rubber contents (above 15% by mixture weight) the soil/rubber solid matrix is significantly controlled by the synthetic portion. The transformation from sand-like to rubber-like behavior is also affected by the relative size of soil versus rubber solids, expressed as $D_{50,s}/D_{50,r}$. The increase of rubber-to-rubber interfaces is more pronounced as the ratio $D_{50,s}/D_{50,r}$ increases. Consequently, the analysis of the results should consider the grain-size characteristics of both the physical and the synthetic portion of the mixtures.
- Using the well-known modified hyperbolic model commonly used for typical soils, analytical equations were proposed for the estimation of the normalized shear modulus as a function of the shearing strain amplitude, γ, the confining pressure, σ'_m, the content of rubber, pr, the grain size characteristics of the physical portion of the mixtures and the relative size of soil versus rubber solids.
- DT–log γ curves were analyzed in terms of correlating the G/G_O with the corresponding DT–DT_O values, where DT_O is the small-strain damping ratio. The normalization of damping ratio in terms of DT–DT_O eliminates the effect of DT_O and thus, the effect of rubber content on the experimental results.
- On the framework of this paper, design G/G_O–log γ and DT–log γ curves for SRM and GRM were also presented for variable rubber contents and confining pressures. It is concluded that for the accurate estimation of the non-linear response of granular soil/rubber mixtures, and thus, for the accurate seismic design of a structure or geo-structure where SRM or GRM is used, it is important to account the effect of the content of rubber, the confining pressure and the relative size of soil versus rubber solids.
- The equations proposed on the framework of this study for the estimation of the strain-dependent shear modulus and damping ratio of the SRM and GRM using simple analytical models were derived from torsional resonant column test data in a range of shearing strain amplitudes from 2×10^{-4}% to 3×10^{-1}%. Consequently, further research is needed on this topic, in order to investigate experimentally the G/G_O–log γ–DT curves of the SRM and GRM at shear strain amplitudes in the order of 1% or higher, which strain amplitudes are of interest under strong earthquake events.
- In future studies, the experimental results of this work could be enriched with additional laboratory tests using cyclic triaxial and/or torsional shear devices in order to study the effect of the number of cycles and the loading frequency on the dynamic response of the SRM and GRM, a topic not covered yet in the literature. In addition, the experimental results of this work could be extended in the future to a wider range of the ratio $D_{50,s}/D_{50,r}$ (mean grain size of soil versus rubber solids) using large-scale resonant column and/or cyclic triaxial devices where specimens of higher diameter in the order of 150–300 mm may be tested.

Acknowledgments

The authors would like to thank the anonymous reviewers for their constructive comments and their detailed suggestions which helped us to improve the quality of the paper.

References

[1] Bosscher P, Edil T, Kuraoka S. Design of highway embankments using tire chips. Journal of Geotechnical and Geoenvironmental Engineering, ASCE 1997;123(4):295–304.

[2] Humphrey D, Whetten N, Weaver J, Recker K, Cosgrove T. Tire shreds as lightweight fill for embankments and retaining walls. In: Vipulanandan C, Elton DJ, editors. Boston, Mass., 18–21 October, 1998 Recycled materials in geotechnical

applications: proceedings of sessions of geo-congress 98. New York: American Society of Civil Engineers; 1998. p. 51–65. [Geotechnical Special Publication 79].
[3] Humphrey D. Effectiveness of design guidelines for use of tire derived aggregate as lightweight embankment fill. Recycled materials in geotechnics 2004;127:61–74.
[4] Humphrey D. Tire derived aggregate as lightweight fill for embankments and retaining walls. In: Hazarika, Yasuhara, editors. 23–24 March 2007, Yokosuka, Japan Proceedings of the international workshop on scrap tire derived geomaterials—opportunities and challenges. London: Taylor & Francis Group; 2007. p. 59–81.
[5] Zornberg J, Christopher B, LaRocque C. Applications of tire bales in transportation projects. Recycled materials in geotechnics 2004;127:42–60.
[6] Edeskar T. Use of tyre shreds in civil engineering applications: technical and environmental properties. PhD dissertation, Lulea University of Technology; 2006.
[7] Karmokar A. Use of scrap tire derived shredded geomaterials in drainage application. In: Hazarika, Yasuhara, editors. 23–24 March 2007, Yokosuka, Japan Proceedings of the international workshop on scrap tire derived geomaterials—opportunities and challenges. London: Taylor & Francis Group; 2007. p. 127–38.
[8] Hall T. Reuse of shredded tire material for leachate collection systems. In: Proceedings of the 14th annual madison waste conference, Department of Engineering Professional Development, University of Wisconsin-Madison; 1991.
[9] Humphrey D, Manion W. Properties of tire chips for lightweight fill. In: Grouting, soil improvement and geosynthetics, Geotechnical Special Publication, American Society of Civil Engineers, New York, vol. 2(30); 1992. p. 1344–55.
[10] Humphrey D, Sandford T, Cribbs M, Manion W. Shear strength and compressibility of tire chips for use as retaining wall backfill. Report, lightweight artificial and waste materials for embankments over soft soils, transportation research record 1422, Transportation Research Board, Washington, DC; 1993. p. 29–35.
[11] Edil T, Bosscher P. Engineering properties of tire chips and soil mixtures. Geotechnical Testing Journal 1994;17(4):453–64.
[12] Masad E, Taha R, Ho C, Papagiannakis T. Engineering properties of tire/soil mixtures as a lightweight fill material. Geotechnical Testing Journal 1996;19(3):297–304.
[13] Foose G, Benson C, Bosscher P. Sand reinforced with shredded waste tires. Journal of Geotechnical Engineering 1996;122(9):760–7.
[14] Tatlisoz N, Benson C, Edil T. Effect of fines on mechanical properties of soil-tire chip mixtures. Testing Soil Mixed With Waste or Recycled Materials 1997:93–108.
[15] Lee J, Salgado R, Bernal A, Lovell C. Shredded tires and rubber–sand as lightweight backfill. Journal of Geotechnical and Geoenvironmental Engineering 1999;125(2):132–41.
[16] Edincliler A, Baykal G, Dengili K. Determination of static and dynamic behaviour of waste materials. Resources, Conservation and Recycling 2004;42(3):223–37.
[17] Edincliler A. Using waste tire-soil mixtures for embankment construction. In: Hazarika, Yasuhara, editors. 23–24 March 2007, Yokosuka, Japan Proceedings of the international workshop on scrap tire derived geomaterials—opportunities and challenges. London: Taylor & Francis Group; 2007. p. 319–28.
[18] Zornberg J, Carbal A, Viratjandr C. Behaviour of tire shred-sand mixtures. Canadian Geotechnical Journal 2004;41:227–41.
[19] Kim H. Spatial variability in soils: stiffness and strength. PhD dissertation, Georgia Institute of Technology, 2005.
[20] Kim H, Santamarina J. Sand–rubber mixtures (large rubber chips). Canadian Geotechnical Journal 2008;45:1457–65.
[21] Promputthangkoon P, Hyde A. Compressibility and liquefaction potential of rubber composite soils. In: Hazarika, Yasuhara, editors. 23–24 March 2007, Yokosuka, Japan Proceedings of the international workshop on scrap tire derived geomaterials—opportunities and challenges. London: Taylor & Francis Group; 2007. p. 161–70.
[22] Hazarika H. Structural stability and flexibility during earthquakes using tyres (SAFETY)—a novel application for seismic disaster mitigation. In: Hazarika, Yasuhara, editors. 23–24 March 2007, Yokosuka, Japan Proceedings of the international workshop on scrap tire derived geomaterials—opportunities and challenges. London: Taylor & Francis Group; 2007. p. 115–25.
[23] Hazarika H, Yasuhara K, Karmokar A, Mitarai Y. Shaking table test on liquefaction prevention using tire chips and sand mixture. In: Hazarika, Yasuhara, editors. 23–24 March 2007, Yokosuka, Japan Proceedings of the international workshop on scrap tire derived geomaterials—opportunities and challenges. London: Taylor & Francis Group; 2007. p. 215–22.
[24] Uchimura T, Chi N, Nirmalan S, Sato T, Meidani M, Towhata I. Shaking table tests on effect of tire chips and sand mixture in increasing liquefaction resistance and mitigating uplift of pipe. In: Hazarika, Yasuhara, editors. 23–24 March 2007, Yokosuka, Japan Proceedings of the international workshop on scrap tire derived geomaterials—opportunities and challenges. London: Taylor & Francis Group; 2007. p. 179–86.
[25] Hyodo M, Yamada S, Orense R, Okamoto M, Hazarika H. Undrained cyclic shear properties of tire chip-sand mixtures. In: Hazarika, Yasuhara, editors. 23–24 March 2007, Yokosuka, Japan Proceedings of the international workshop on scrap tire derived geomaterials—opportunities and challenges. London: Taylor & Francis Group; 2007. p. 187–96.
[26] Tsang H-H. Seismic isolation by rubber–soil mixtures for developing countries. Earthquake Engineering and Structural Dynamics 2008;37:283–303.
[27] Kaneda K, Hazarika H, Yamazaki H. The numerical simulation of earth pressure reduction using tire chips in backfill. In: Hazarika, Yasuhara, editors. 23–24 March 2007, Yokosuka, Japan Proceedings of the international workshop on scrap tire derived geomaterials—opportunities and challenges. London: Taylor & Francis Group; 2007. p. 245–51.
[28] Takatani T. Seismic response analysis of caisson quay wall reinforced with protective cushion. In: Hazarika, Yasuhara, editors. 23–24 March 2007, Yokosuka, Japan Proceedings of the international workshop on scrap tire derived geomaterials—opportunities and challenges. London: Taylor & Francis Group; 2007. p. 229–38.
[29] Senetakis K, Anastasiadis A, Trevlopoulos K, Pitilakis K. Dynamic response of SDOF systems on soil replaced with sand/rubber mixture. In: Proceedings of the ECOMAS thematic conference on computation methods in structural dynamics and earthquake engineering, June 22–24, Rhodes, Greece; 2009.
[30] Mavronicola E, Komodromos P, Charmpis D. Numerical investigation of potential usage of rubber–soil mixtures as a distributed seismic isolation approach. In: Topping BHV, Adam JM, Pallarés FJ, Bru R, Romero ML, editors. Proceedings, Tenth International Conference on Computational Structures Technology. Stirlingshire, UK: Civil-Comp Press; 2010, doi:10.4203/ccp.93.168. [Paper 168].
[31] Pitilakis K, Trevlopoulos K, Anastasiadis A, Senetakis K. Seismic response of structures on improved soil. In: Proceedings of the eighth international conference on structural dynamics (EURODYN2011Q2). 4–6 July Leuven. Belgium; 2011.
[32] Feng Z-Y, Sutter K. Dynamic properties of granulated rubber/sand mixtures. Geotechnical Testing Journal 2000;23(3):338–44.
[33] Anastasiadis A, Pitilakis K, Senetakis K. Dynamic shear modulus and damping ratio curves of sand/rubber mixtures. In: Proceedings of the earthquake geotechnical engineering satellite conference, XVIIth international conference on soil mechanics & geotechnical engineering, October 2–3, Alexandria, Egypt; 2009.
[34] Senetakis K, Anastasiadis A, Pitilakis K, Souli A. Dynamic behavior of sand/rubber mixtures, Part II: effect of rubber content on G/G_O–γ–DT curves and volumetric threshold strain. Journal of ASTM International 2012;9:2.
[35] Senetakis K, Anastasiadis A, Pitilakis K. Experimental investigation of the dynamic properties of granular soil/rubber mixtures using a resonant column device. In: Proceedings of the fifth international conference on earthquake geotechnical engineering, January 10–13, Santiago, Chile; 2011.
[36] Senetakis K. Dynamic properties of granular soils and mixtures of typical sands and gravels with recycled synthetic materials. PhD Dissertation, Department of Civil Engineering, Aristotle University of Thessaloniki, Greece (in Greek); 2011.
[37] Anastasiadis A, Senetakis K, Pitilakis K, Gargala C, Karakasi I. Dynamic behavior of sand/rubber mixtures, Part I: effect of rubber content and duration of confinement on small-strain shear modulus and damping ratio. Journal of ASTM International 2012;9:2.
[38] Anastasiadis A, Senetakis K, Pitilakis K. Small strain shear modulus and damping ratio of sand/rubber and gravel/rubber mixtures. Journal of Geotechnical and Geological Engineering, in press.
[39] ASTM. Standard practice for classification of soils for engineering purposes (Unified Soil Classification System): D2487-00. In: Annual book of ASTM standards, ASTM International; 2000.
[40] ASTM. Standard practice for use of scrap tires in civil engineering applications: D6270-98. In: Annual book of ASTM standards, ASTM International; 1998.
[41] ASTM. Standard test methods for specific gravity of soil solids by water pycnometer: D854-02. In: Annual book of ASTM standards, ASTM International; 2002.
[42] Drnevich V. Effects of strain history on the dynamic properties of sand, PhD dissertation, University of Michigan; 1967.
[43] ASTM. Standard test methods for modulus and damping of soils by the resonant column method: D4015-92. In: Annual book of ASTM standards, ASTM International; 1992.
[44] Anastasiadis A, Pitilakis K, Senetakis K, Souli A. Dynamic response of sandy and gravelly soils: Effect of grain size characteristics on G–γ–D curves. In: Proceedings of the fifth international conference on earthquake geotechnical engineering, January 10–13, Santiago, Chile; 2011.
[45] Menq F-Y. Dynamic properties of sandy and gravelly soils. PhD dissertation, University of Texas at Austin; 2003.
[46] Seed H, Wong R, Idriss I, Tokimatsu K. Moduli and damping factors for dynamic analysis of cohesionless soils. Journal of Geotechnical Engineering, ASCE 1986;112(11):1016–103.
[47] Stokoe K, Darendeli M, Andrus R, Brown LT. Dynamic soil properties: laboratory, field and correlation studies. In: Proceedings of the second international conference on earthquake geotechnical engineering, Lisbon; 1997.
[48] Darendeli M. Dynamic properties of soils subjected to 1994 Northridge earthquake. M.S. Dissertation, University of Texas at Austin; 1999.
[49] Darendeli M. Development of a new family of normalized modulus reduction and material damping curves, PhD Dissertation, University of Texas at Austin, 2001.